



# VCU

Virginia Commonwealth University  
VCU Scholars Compass

---

Theses and Dissertations

Graduate School

---

2009

## Ion Channel Modulation by Photocaged Dioctanoyl PIP2

Junghoon Ha

*Virginia Commonwealth University*

Follow this and additional works at: <https://scholarscompass.vcu.edu/etd>



Part of the [Physiology Commons](#)

© The Author

---

Downloaded from

<https://scholarscompass.vcu.edu/etd/1930>

This Thesis is brought to you for free and open access by the Graduate School at VCU Scholars Compass. It has been accepted for inclusion in Theses and Dissertations by an authorized administrator of VCU Scholars Compass. For more information, please contact [libcompass@vcu.edu](mailto:libcompass@vcu.edu).

# **ION CHANNEL MODULATION BY PHOTOCAGED DIOCTANOYL PIP<sub>2</sub>**

A thesis submitted in partial fulfillment of the requirements for the degree of Master of Science  
at Virginia Commonwealth University

by

JUNGHOON HA  
BSc. University of Virginia, Charlottesville, VA, 2004

Thesis Director: DIOMEDES E. LOGOTHETIS  
CHAIR, DEPARTMENT OF PHYSIOLOGY AND BIOPHYSICS

Virginia Commonwealth University  
Richmond, Virginia  
August, 2009

## ACKNOWLEDGEMENT

First and foremost, I would like to thank my thesis mentor, Dr. Diomedes Logothetis. Without his guidance and leadership, I would not have been so eager to pursue a career in becoming a physician-scientist. He has been absolutely supportive in the face of any hardships I've encountered in the past year, never ceasing to amaze me with his patience and resourcefulness. I would also like to extend my thanks to my committee members, Dr. Clive Baumgarten and Dr. Matthew Hartman, who have been supportive throughout this process. In particular, Dr. Baumgarten has imparted me with an invaluable general overview of ion channels and electrophysiology, and this has enhanced my graduate experience. My gratitude extends to my previous mentors, Dr. Kevin Pfister and Dr. Anthony Spano who have greatly shaped my scientific thinking in the years that I was an undergraduate student and lab technician prior to my enrollment in VCU's graduate program.

I would also like to thank my colleagues and good friends, Frank Chen, Rahul Mahajan, Vasileios Petrou, and Hoon Shim for providing me with tremendous support and enabling me to think critically about my experiments as well as giving me moral support through my personal hurdles. They have challenged my thinking and kept filling me with ideas even during the couple months when the poor oocyte health stymied my research efforts. Especially without Frank Chen and Hoon Shim keeping me company at late hours in the lab, I am certain my laboratory life

would not have sailed as smoothly. I want to thank all of the other laboratory members of the Logothetis lab who were readily available to provide me with technical support and counsel, without whom I would not be able to invest all of my time in to my thesis work as well as freeing me from trouble-shooting. Special thanks goes to Dr. Qiongyao Tang whose expert help proved necessary given the fragility of the oocyte patches to conclude experiments in a timely manner for my Masters dissertation. Special thanks also goes to Dr. Ching-Kang Chen for the use of his hand-held UV lamp for the irradiation experiments.

My life outside of science could not have been as enriched without Jennifer Cole, who has been steadfastly caring and compassionate towards me especially during the most unpredictable phases of my life. She has been nothing but encouraging in my attainment of my ambitions as a physician-researcher as well as this thesis work. My sincere thanks also goes towards Pascal Vicaire, Christopher Nelson, and David Del Vecchio, who despite being separated from me by geography have kept in touch with me on a frequent basis, always sensitive to my general well-being.

Lastly, and most importantly, I would like to thank my parents, Jonghye and Sangdo Ha, my brother, Jayhoon Ha, and my grandparents, Youngbae and Jungho Kim. These are the people who've colored my perspective of the world as well as my personal life. I would also like to acknowledge my aunts, Jongshin and Jongshil Kim who've treated me as if I were their very own son ever since the earliest memories I can conjure up of my childhood. Throughout the small steps I've taken in life, they've shown me it is okay to be human and fall occasionally. Without their unconditional love, I would not be where I am today.

## TABLE OF CONTENTS

	Page
Acknowledgements.....	ii
List of Figures.....	v
List of Abbreviations .....	vii
Abstract.....	ix
Chapter	
1. INTRODUCTION .....	1
2. MATERIALS AND METHODS.....	19
3. RESULTS .....	34
4. DISCUSSION AND FUTURE DIRECTIONS .....	50
5. LITERATURE CITED.....	54
6. VITA.....	57

## LIST OF FIGURES

	Page
Figure 1: Phosphatidylinositol (4,5)-bisphosphate and dioctanoyl PI(4,5)-bisphosphate (diC8) .....	7
Figure 2: Dendrogram of the Kir family .....	9
Figure 3: PIP <sub>2</sub> signaling pathway indirectly modulates ion channels through the activation of protein kinase C (PKC) and Ca <sup>2+</sup> -dependent enzymes using secondary messengers .....	11
Figure 4: Stimulatory effect of PIP <sub>2</sub> on Kir channels via direct regiospecific-electrostatic interactions .....	13
Figure 5: Injection of diC8 into HEK293 cells reduces the inhibitory effect of protein kinase C (PKC) on whole-cell Kir3.1/Kir3.4 activity .....	15
Figure 6: Kir channels have differential apparent affinity to PIP <sub>2</sub> .....	17
Figure 7: A schematic demonstrating inwardly-rectifying whole-cell potassium currents in <i>Xenopus laevis</i> oocytes using the ramp protocol .....	24
Figure 8: A schematic of cell-attached (C/A) and inside-out (I/O) macropatch setup .....	26
Figure 9: Inside-out (I/O) patch gives us external control over cytoplasmic conditions .....	28
Figure 10: Activating photocaged-diC8 with ultraviolet (UV) irradiation .....	30
Figure 11: A schematic of diC8 and singly and doubly photocaged-diC8 .....	32
Figure 12: Expression of Kir2.3 in <i>Xenopus laevis</i> oocytes gives rise to robust whole-cell inwardly rectifying potassium current .....	38

Figure 13: Application of long chain PIP <sub>2</sub> (aa-st PIP <sub>2</sub> ) to the cytoplasmic side of inside-out oocyte macropatch activates the Kir2.3 current.....	40
Figure 14: Application of dioctanoyl PIP <sub>2</sub> (diC8) to the cytoplasmic side of inside-out oocyte macropatch rescues Kir2.3 current.....	42
Figure 15: Preliminary finding shows that caged-diC8 is inactive.....	44
Figure 16. Caged-diC8 activates the Kir2.3 current, while irradiation (de-caging) limits the effectiveness of caged-diC8.....	46
Figure 17: Summary data: caged-diC8 effect before and after UV irradiation .....	48

## LIST OF ABBREVIATIONS

<b>aa-st PIP<sub>2</sub></b>	L- $\alpha$ -phosphatidylinosito-4,5-bisphosphate
<b>C/A</b>	Cell-attached
<b>Caged-diC8</b>	Caged dioctanoyl phosphatidylinositol bisphosphate
<b>cRNA</b>	Complementary ribonucleic acid
<b>DAG</b>	Diacylglycerol
<b>DNA</b>	Deoxyribonucleic acid
<b>DiC8</b>	Dioctanoyl phosphatidylinositol bisphosphate
<b>FVPP</b>	Fluoride/Vanadate/PyroPhosphate
<b>HK</b>	High potassium bath solution
<b>I/O</b>	Inside-out
<b>IP<sub>3</sub></b>	Inositol 1,4,5-trisphosphate
<b>IRK3</b>	Inwardly rectifying potassium channel 3



<b>K<sub>ATP</sub></b>	Adenosine-5'-tri-phosphate activated potassium channel
<b>Kir</b>	Inwardly rectifying potassium channels
<b>MOPS</b>	3-(N-Morpholino)propanesulfonic acid
<b>ND96K</b>	High potassium bath solution
<b>PI</b>	Phosphatidylinositide
<b>PIP5K</b>	Phosphatidylinositol-4-phosphate 5-kinase
<b>PI(4)P</b>	Phosphatidylinosito-4-phosphate
<b>PI(3,4)P<sub>2</sub></b>	Phosphatidylinosito-3,4-bisphosphate
<b>PI(4,5)P<sub>2</sub></b>	Phosphatidylinosito-4,5-bisphosphate
<b>PKC</b>	Protein kinase C
<b>PLC-<math>\gamma</math></b>	Phospholipase C gamma
<b>PMA</b>	Phorbol 12-myristate 13-acetate
<b>PtdIns</b>	Phosphatidylinositol
<b>RNA</b>	Ribonucleic acid
<b>TEVC</b>	Two-electrode voltage clamp
<b>UV</b>	Ultraviolet
<b>WMN</b>	Wortmannin

## ABSTRACT

### ION CHANNEL MODULATION BY PHOTOCAGED DIOCTANOYL PIP<sub>2</sub>

by Junghoon Ha, BSc.

A thesis submitted in partial fulfillment of the requirements for the degree of Master of Science  
at Virginia Commonwealth University.

Virginia Commonwealth University, 2009

Thesis Director: Diomedes E. Logothetis, Ph.D.

Chair, Department of Physiology and Biophysics

Phosphatidylinositol biphosphate (PIP<sub>2</sub>) directly regulates electrophysiological activity in a diverse family of ion channels whether the effect is stimulatory or inhibitory. Much has been unveiled about the apparent affinity and modulatory function of PIP<sub>2</sub> using a chemically

modified dioctanoyl PIP<sub>2</sub> (diC8), a membrane delimited cytosolic co-factor in inside-out macropatch experiments. Yet, the scarcity of molecular tools that permit fine external control in whole-cell systems has precluded future studies from probing the physiological role of PIP<sub>2</sub> in cells in the presence of a fully intact cytoplasm. Here we introduce light as an external control for PIP<sub>2</sub> through photocaging of diC8, and test its activation of Kir2.3 (IRK3), an inwardly rectifying ion channel that has previously shown to possess moderate binding affinity to PIP<sub>2</sub>, in excised, inside-out macropatches. Our experiments revealed that photocaged-diC8 and irradiated photocaged-diC8 have significantly different activation kinetics than the fully active diC8. Surprisingly, the activation of caged-diC8 by UV irradiation attenuated Kir2.3 activity, while the inactivated diC8 (caged-diC8) resulted in similar magnitude of channel activity compared to the currents elicited by unmodified diC8. Interestingly, we also show that application of both activated (irradiated) and inactive (caged) diC8 in macropatches generated highly fluctuating ion channel activity.

## INTRODUCTION

Ion channels, macromolecular pores in cell membranes that belong to a diverse family, are regulated by complex extracellular and intracellular signals. Most notably, it is their concerted response that allows our cells to communicate in a coordinated manner through electrical signals in nerves, muscles, and synapses. This coordinated electrical activity equips us with the ability to perceive and react immediately to changes in our environment. Garnering much attention in science, great progress has been made in the past several decades to aid our understanding of this remarkable family of proteins. Initially, ion channels were successfully characterized as pores in lipid membranes. Soon after, their contribution to an electrochemical gradient across the plasma membrane (along with transporters) as well as the complex nature of the membrane spanning channels became the focus of many researchers (10). Breakthrough electrophysiological techniques such as patch clamping have greatly shaped and contributed to our current understanding of ion channel function (7).

In particular, with powerful and versatile experimental tools that became available with the advent of patch clamp, researchers have been able to determine over the past 30 years key co-factors of ion channel regulation. In parallel to the discovery and characterization of complex

cytoplasmic modulators and their effector ion channels, inside-out patch experiments on inwardly rectifying potassium (Kir) channels have led to the discovery of a myriad of cytoplasmic modulators of ion channel function and most notably lipid-induced gating of channels (such as that induced by  $\text{PIP}_2$  – Fig. 1). While previous studies on ion channels searched solely for proteins that interact with ion channels, Hilgemann and colleagues demonstrated that phosphoinositides, highly negative-charged anionic lipids with myo-inositol in the head group can also directly modulate channel activity (9). Their experiments revealed that phosphoinositides such as phosphatidylinositol-4,5-bisphosphate ( $\text{PIP}_2$ ) can activate native cardiac  $\text{K}_{\text{ATP}}$  channels. Ensuing studies by Fan and Makielski uncovered that  $\text{PIP}_2$  modulation of ion channels was not only limited to  $\text{K}_{\text{ATP}}$  channels, but also applied to other inwardly rectifying potassium (Kir) channels such as Kir1.1 and Kir2.1 (5). In the past decade, experiments that focused on  $\text{PIP}_2$  modulation of inwardly rectifying potassium (Kir) channels have revealed that virtually all members of the Kir channel family [Fig. 2] are affected by  $\text{PIP}_2$  and eventually served as paradigm to probe other ion channel- $\text{PIP}_2$  interactions (13). In agreement with studies on Kir channels,  $\text{PIP}_2$  has emerged as an ubiquitous modulator of ion channel and transporter function (18).

Thereby, phosphatidylinositol-4,5-bisphosphate,  $\text{PI}(4,5)\text{P}_2$ , was shown to be the most abundant and potent of the phosphoinositides in Kir channel modulation compared to other naturally occurring phosphoinositides: PI,  $\text{PI}(4)\text{P}$ ,  $\text{PI}(3,4)\text{P}_2$ ,  $\text{PI}(3,5)\text{P}_2$  and  $\text{PI}(3,4,5)\text{P}_3$  (8, 14, 19, 20). Although, the parent compound phosphatidylinositol (PI) can become phosphorylated at the 3, 4, and 5 positions of the inositol ring in every combination,  $\text{PI}(4,5)\text{P}_2$  [Fig. 1] is the most abundant poly-phosphoinositol making up 1% of the total phospholipids of the plasma membrane (6).  $\text{PIP}_2$  has three phosphate groups, one of which is in a phosphodiester bond, and a

net charge near -5 at neutral pH (12). In the late 1970s, PIP<sub>2</sub> was shown to be the substrate of plasma membrane-delimited enzyme phospholipase C (PLC), which hydrolyzes PIP<sub>2</sub> into two secondary messengers [Fig. 3], soluble inositol 1,4,5-trisphosphate (IP<sub>3</sub>) and membrane-anchored diacylglycerol (DAG) (18). IP<sub>3</sub> and DAG were subsequently shown to release Ca<sup>2+</sup> from intracellular stores within the cell and to recruit and activate protein kinase C (PKC), respectively (12). Moreover, PIP<sub>2</sub> was shown to serve as a targeting anchor for proteins that catalyze endocytosis and exocytosis such as GTPases, PKC, and other components of the actin cytoskeleton (18). Since PIP<sub>2</sub> served as an epicenter for these two signaling pathways that affect ion channel function indirectly through secondary messengers, it became critical to perform the necessary control experiments to ensure that electrical phenotype was a result of direct PIP<sub>2</sub>-channel interactions.

As it became increasingly evident that PIP<sub>2</sub> is requisite for ion channel and transporter function in the plasma membrane, laboratories began focusing on where and how PIP<sub>2</sub> interacts with Kir channels. First attempts examined the effects of naturally occurring phosphoinositol lipids on cloned Kir6.2/SUR1, through their direct application to the cytoplasmic membrane side of excised patches (19). In these experiments, channel activity was allowed to rundown, a process which typically occurs in excised patches due to hydrolysis and dephosphorylation of endogenous phosphoinositides. Then PIP<sub>2</sub> as well as various phosphoinositides were tested to see whether they could restore channel function.

As PIP<sub>2</sub> emerged as the most effective of the phosphoinositides in recovering (activating) channel activity, it became clear that Kir channels exhibited distinct regiospecificities of interaction with the phosphate groups on inositol carbon positions 4 and 5 (13). Hypothesizing

that PIP<sub>2</sub>'s acidic negatively charged phosphates (at neutral pH) interact electrostatically with basic positively charged residues on ion channels [Fig. 4], laboratories focused on identifying channel regions that are vital for ion-channel modulation by PIP<sub>2</sub>. These inside-out patch experiments required the use of modified shorter PIP<sub>2</sub> analogs such as dioctanoyl PIP<sub>2</sub> (diC8), which due to their water solubility were much easier to wash out of membranes (13). Logothetis and coworkers utilized diC8 to determine the apparent affinity of PIP<sub>2</sub> for a particular Kir channel and compare it to other channels. (16, 17).

The conserved basic sites that bind PIP<sub>2</sub> were unveiled through systematic mutagenesis of highly conserved basic residues in the cytoplasmic domains of Kir channels (13). Mutant channels, whose basic residues were replaced with neutral residues, exhibited decreased recovery of ion channel activity upon addition of exogenous PIP<sub>2</sub> to the cytoplasmic side. Furthermore, mutant channels showed increased sensitivity to inhibition by poly-L-lysine (a PIP<sub>2</sub> scavenger) as well as PIP<sub>2</sub> specific antibodies suggesting that the mutations reduced apparent PIP<sub>2</sub> affinity (22). Subsequent experiments also showed that one could swap a mere residue in Kir2.3 with a corresponding residue in a related Kir channel (Kir2.1) [Fig. 6] that is more sensitive to PIP<sub>2</sub>, to increase its apparent affinity to PIP<sub>2</sub> and vice-versa (4).

Thus, our understanding of ion channel modulation by PIP<sub>2</sub> has offered great insights into mechanisms underlying the gating of ion channels. However, PIP<sub>2</sub> regulation of ion channels in more physiological whole-cell systems (as opposed to the excised patch setting which is removed from a constellation of known and putative cytoplasmic co-factors), still greatly eludes us. Heterologous systems (such as *Xenopus laevis* oocytes used to study ion channel modulation) fall short as models of specialized excitable cells and, thus are not as useful in evaluating PIP<sub>2</sub>'s

physiological significance in cellular function; PIP<sub>2</sub>'s effects must be verified in native cells. Keselman and colleagues have loaded soluble diC8 into a whole cell through the electrode tip (11). Although, the loading of PIP<sub>2</sub> produced the predicted effect, attenuating the inhibitory effect of protein kinase C (PKC) on Kir3.1/Kir3.4 channels by replacing hydrolyzed PIP<sub>2</sub> at the plasma membrane [Fig. 5], the method is in reality a crude approximation of the effect of PIP<sub>2</sub> on ion channels in whole-cell systems. The delivery of diC8 into the whole cell through the electrode tip presents numerous seemingly insurmountable limitations. The diffusion of PIP<sub>2</sub> becomes a significant artificial determinant influencing the modulation of ion channels. In the course of diffusion, PIP<sub>2</sub> may stick to the walls of the glass electrode and could also be rapidly quenched by cytoplasmic enzymes. Such possibilities are of concern especially as indicated by the fact that large concentrations of PIP<sub>2</sub> are required in the electrode (e.g. 200 μM) to elicit a significant PIP<sub>2</sub> response. Such concentrations can be 1-2 orders of magnitude higher than has been convincingly shown in excised patch experiments. The total estimate of PIP<sub>2</sub> in a whole cell is thought to be equivalent to a 4-10 μM solution if dissolved in the cytoplasm (14). Greater external control over diC8 is required to improve the delivery of PIP<sub>2</sub> in whole-cell experiments that aim to evaluate physiological effects of known PIP<sub>2</sub> concentrations.

To this cause, chemically modifying diC8 (PIP<sub>2</sub> analogs) constitutes a novel attempt to improve the delivery of PIP<sub>2</sub> into whole-cell systems. In a process called "photocaging," one can shield the active domains of PIP<sub>2</sub>, through the addition of effective "caging groups" such as 2-nitrobenzyl group I and the coumarin moiety (21). Ultraviolet (UV) light would then be applied to activate the caged molecule at a specific wavelength. Nitrobenzyl groups have been installed on small inducers of gene expression, such as doxycycline, tetracycline, lactose, β-estradiol, and ecdysone, in order to cage and inactivate these molecules (1, 2, 12, 15). When these caged

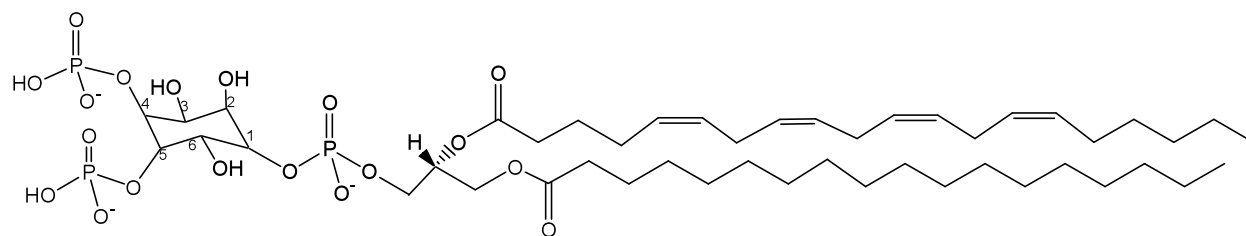


inducers are irradiated at their maximum absorption wavelength and freed from the “caging,” they are able to bind the protein activator, which binds to a promoter sequence on DNA, turning on gene expression. Experiments with fluorescent reporters have already demonstrated the spatio-temporal control one can exert on systems using light and photocaged molecules (21). Commonly, the photocages are decorated with electron donating groups (-OCH<sub>3</sub>) to shift the maximum adsorption to a longer wavelength (365 nm) to avoid damaging the cells as well as activating several UV-induced signaling pathways (21).

With the ultimate aim to better understand the physiological role of PIP<sub>2</sub> in a whole-cell system, we are collaborating with Dr. Deiters and his coworkers who have synthesized and provided us with a mixture of photocaged diC8, adding nitrobenzyl groups as cages to phosphate groups on the inositol head group at either positions 4 or 5 or simultaneously at both positions [Fig. 11]. Prior to using the photocaged dioctanoyl PIP<sub>2</sub> (diC8) on whole-cell systems, we have concentrated on testing the effect of photocaged-diC8 on *Xenopus laevis* oocyte macropatches containing Kir2.3 channels that have moderate apparent affinity [Fig. 6] to diC8 among inwardly rectifying potassium channels (in comparison to the high affinity Kir2.1 and the low affinity Kir3.x channels).

**Figure 1. Phosphatidylinositol (4,5)-bisphosphate and dioctanoyl PI(4,5)-bisphosphate (diC8).** PtdIns(4,5)P<sub>2</sub> is a minor phospholipid component of the cytoplasmic leaflet in plasma membranes, where it is a significant substrate for a number of membrane-localized signaling proteins. PtdIns(4,5)P<sub>2</sub> is primarily made by the type I phosphatidylinositol 4 phosphate 5 kinases from PI(4)P. **A. Long-chain aa-st PI(4,5)P<sub>2</sub>.** Schematic of endogenously produced PI(4,5)P<sub>2</sub>. **B. Soluble dioctanyl PI(4,5)P<sub>2</sub> (diC8).** Schematic of chemically modified PI(4,5)P<sub>2</sub>. The palmitoyl group and 19-carbon long chain of aa-st PI(4,5)P<sub>2</sub> have been replaced by shorter, more soluble singly-bonded 8-carbon long fatty acid chains.

A. Long chain PIP<sub>2</sub> (aa-st PIP<sub>2</sub>)



B. Dioctanoyl PIP<sub>2</sub> (diC8)

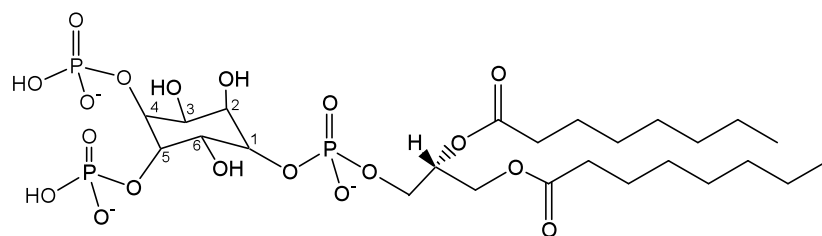


**Figure 2. Dendrogram of the Kir family.** The Kir superfamily contains at least 15 members in six distinct subfamilies (Kir1, Kir2, Kir3, Kir5, Kir6, Kir7) that respond to various cytoplasmic and extracellular modulators; channels are two-membrane spanning (2TM) and share about 30-40% homology among the Kir subfamilies and >60% within the subfamilies. Kir channels were characterized strictly by their electrophysiological behavior as they allow more conduction in the inward than in the outward direction due to reduced open probability in depolarizing conditions across the membrane. However, in physiological conditions, Kir channels have a key role in stabilizing the membrane potential. In addition, regulation of these channels can alter the membrane potential and cellular excitability.

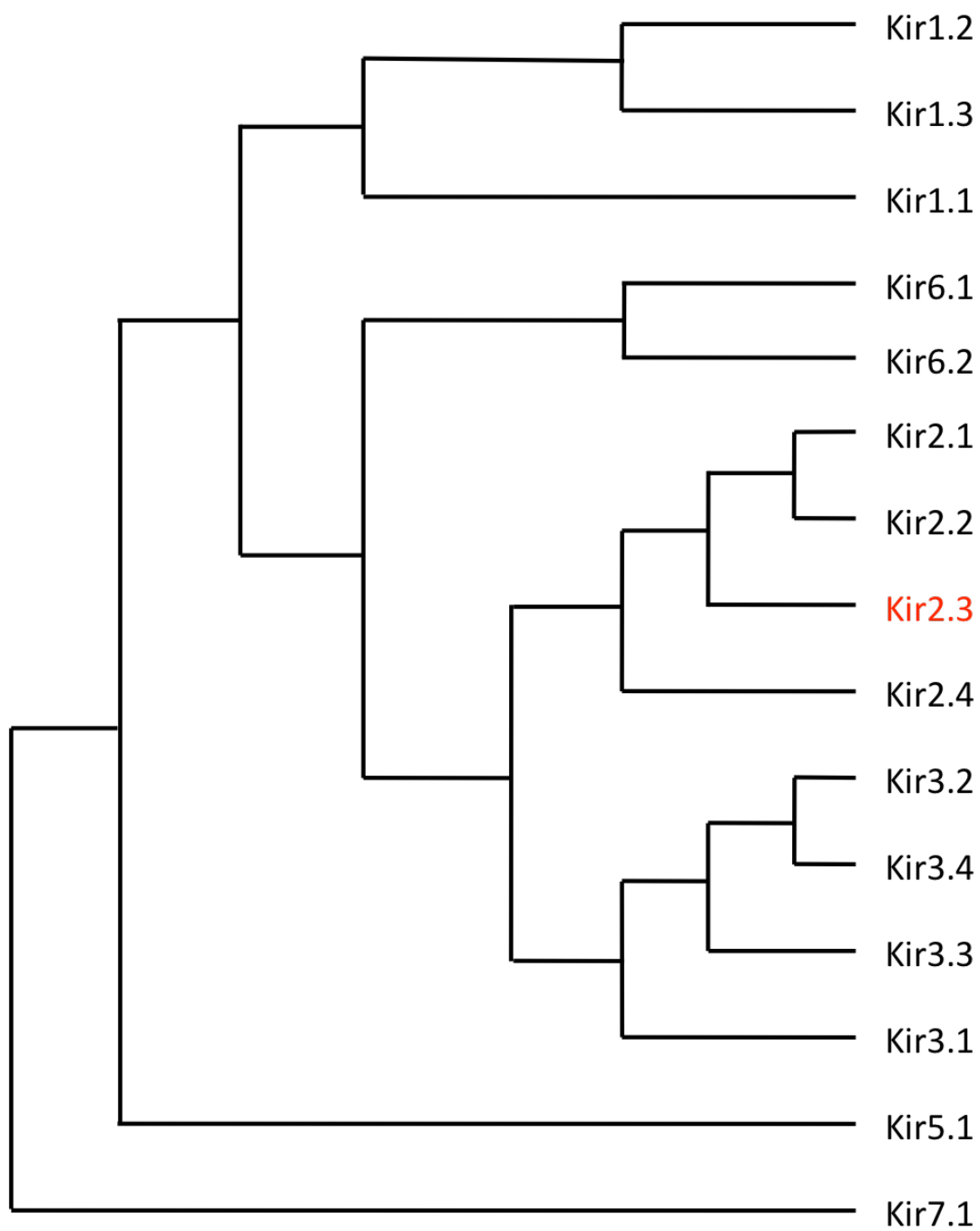


**Figure 3. PIP<sub>2</sub> signaling pathway indirectly modulates ion channels through the activation of protein kinase C (PKC) and Ca<sup>2+</sup>-dependent enzymes using secondary messengers.**

Activation of phospholipase C (PLC) results in the hydrolysis of phosphatidylinositol (PIP<sub>2</sub>) to produce inositol 1,4,5-triphosphate (IP<sub>3</sub>) and diacylglycerol (DAG). IP<sub>3</sub> activates Ca<sup>2+</sup> channels in the endoplasmic reticulum (ER) triggering the release of Ca<sup>2+</sup> from intracellular stores. The cytoplasmic rise in Ca<sup>2+</sup> level and DAG then activate protein kinase C (PKC), which in turn phosphorylates K<sup>+</sup> channels, thereby modulating current across the membrane.

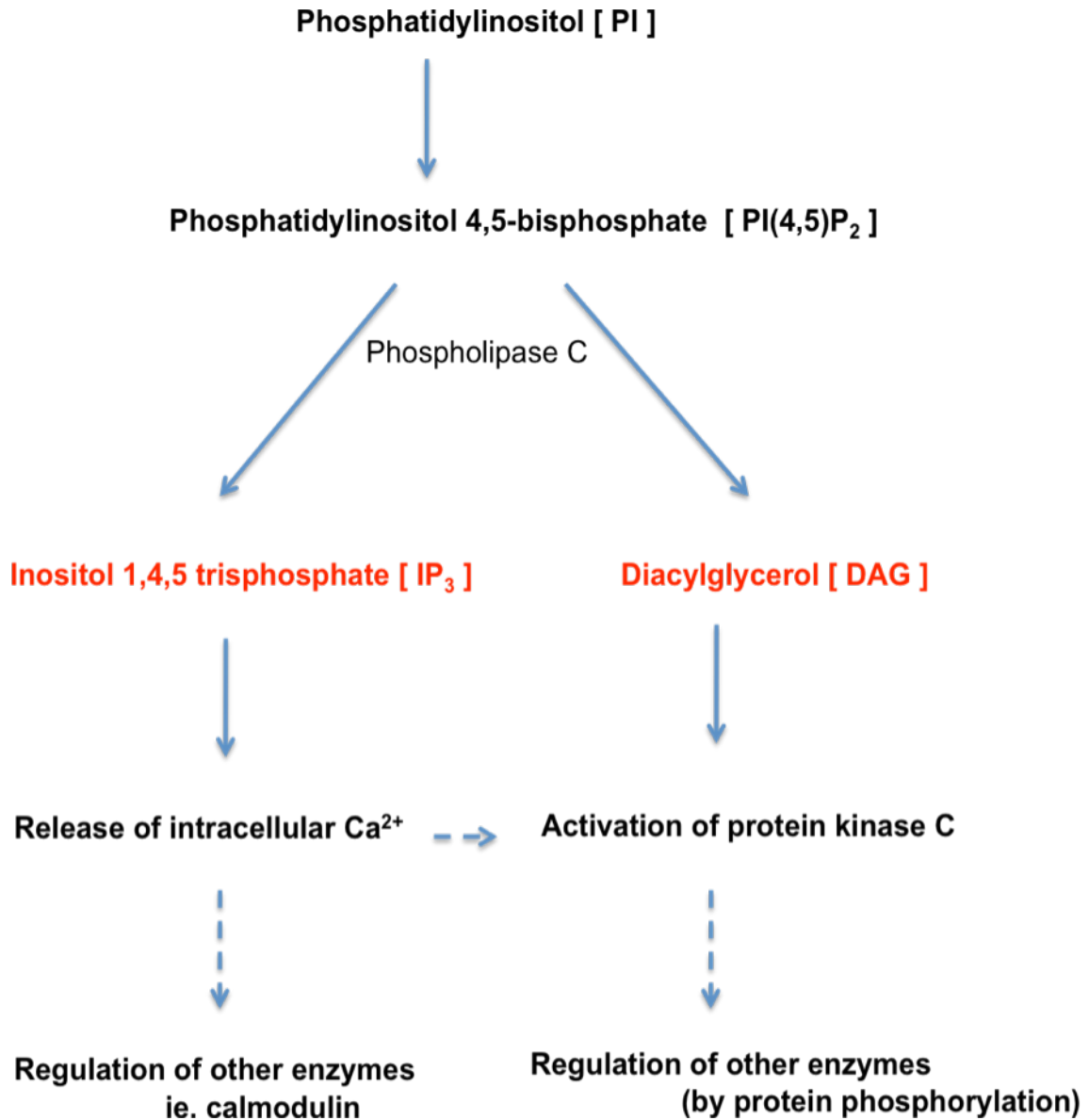
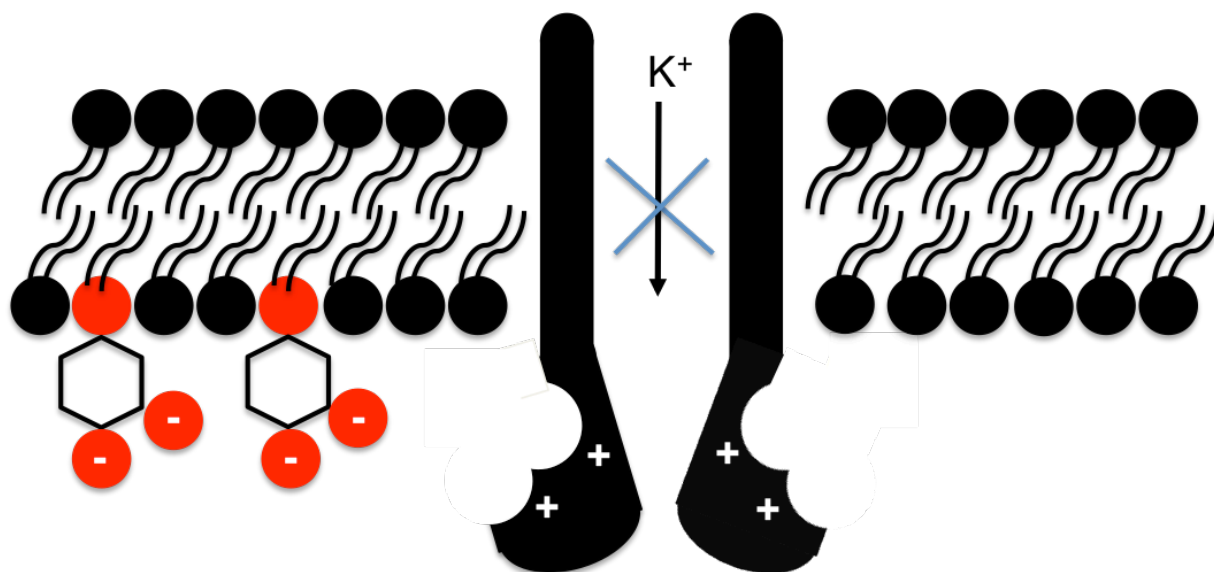


**Figure 4. Stimulatory effect of PIP<sub>2</sub> on Kir channels via direct regiospecific-electrostatic interactions.** Two highly negative-charged phosphate groups (depicted here by red circles) attached to the 4 and 5 carbons of inositol (represented by hexagonal inositol ring) in the inner leaflet of the plasma membrane interact with candidate positively charged residues that are highly conserved in the Kir superfamily. Net inward movement of potassium ions depicted by the blue arrow is indicative of hyperpolarizing conditions typically applied to membranes expressing Kir channels. **A.** Schematic of a Kir channel in the inactivated closed state. When the level of PIP<sub>2</sub> is low (often depleted through PIP<sub>2</sub> dephosphorylation, hydrolysis, or run down in excised patch experiments), Kir channel remains in the closed state. **B.** Schematic of a Kir channel in the activated open state via the binding of PIP<sub>2</sub> to the channel: relies both on the spatial distribution of phosphate groups on the inositol ring as well as electrostatic interactions.



A.



B.

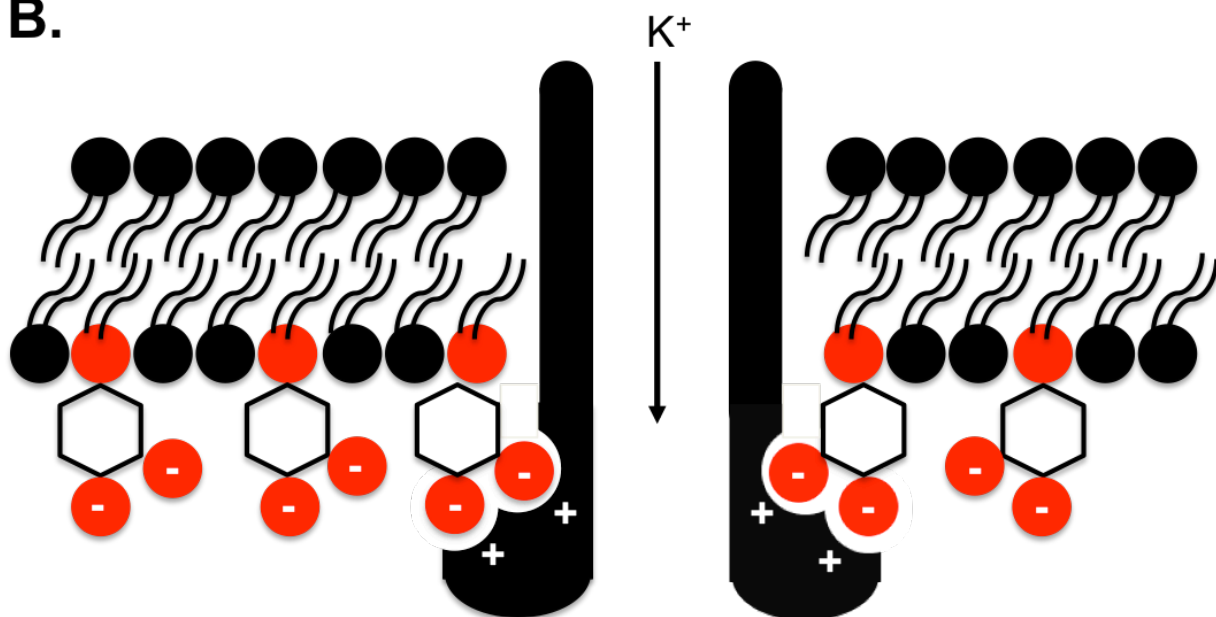


**Figure 5. Injection of diC8 into HEK293 cells reduces the inhibitory effect of protein kinase C (PKC) on whole-cell Kir3.1/Kir3.4 activity.** Figure is taken from Keselman, *et al.* [17]. Activation of PKC with phorbol 12-myristate 13-acetate (PMA) inhibits whole-cell Kir3.1/Kir3.4 activity. Applying PMA and inducing PIP<sub>2</sub> hydrolysis using wortmannin (WMN), a fungal metabolite that serves to deplete whole cell-PIP<sub>2</sub> levels (at micromolar concentration) both serves to inhibit the activity of Kir3.1/Kir3.4 channels. On the other hand, addition of PIP5K (in addition to PMA), which should increase the whole-cell PIP<sub>2</sub>, countered the inhibitory effect of PMA on Kir3.1/Kir3.4 activity. Lastly, application of dioctanoyl PIP<sub>2</sub> (diC8) at 200  $\mu$ M concentration through the electrode rescued Kir3.1/Kir3.4 activity from the inhibitory effect of PMA.

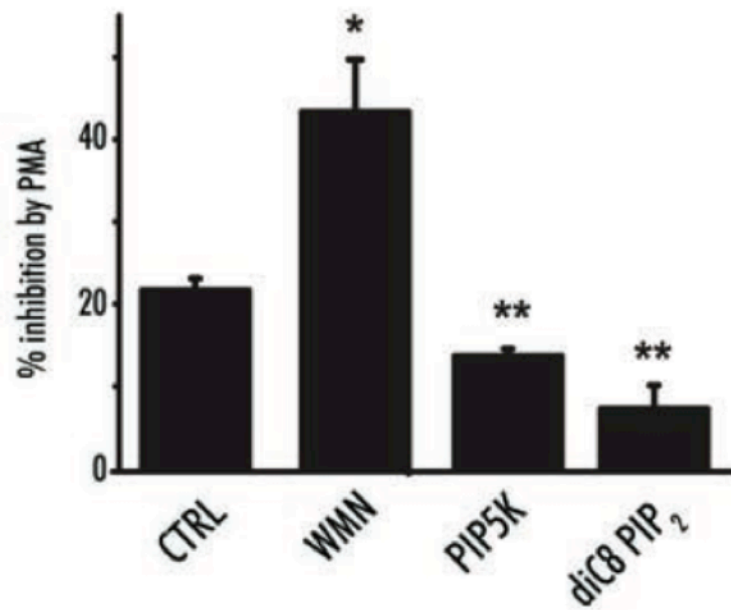
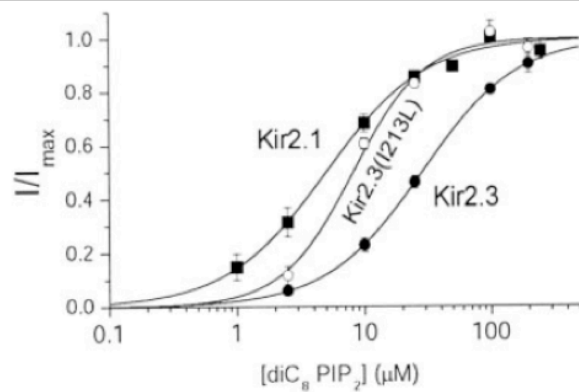


**Figure 6. Kir channels have differential apparent affinity to PIP<sub>2</sub>.** Figure is taken from Du, *et al.* [16]. Inwardly rectifying potassium channels have distinct sensitivities to PIP<sub>2</sub>: for example, Kir 2.1 is approximately one order of magnitude more sensitive to PIP<sub>2</sub> than Kir2.3. Replacing a single residue in Kir2.3 with a corresponding residue in Kir 2.1 (I to L), a channel that binds with higher affinity to PIP<sub>2</sub>, significantly increases the apparent affinity of Kir2.3 to PIP<sub>2</sub>. **Left Panel:** One residue that significantly affects Kir-PIP<sub>2</sub> interaction is highlighted across the superfamily of Kir channels (L, I, M, or V). **Right Panel:** Dose response curves constructed from measurements of inside-out macropatches expressing the channels indicated (Kir2.1, Kir2.3, and Kir2.3-I213L) in *Xenopus laevis* oocytes respond to different concentrations of diC8. Swapping a single isoleucine (I) residue in Kir2.3 with a corresponding leucine (L) residue in Kir2.1 makes it approximately 5 times more sensitive to diC8.

Kir1.1	217	RKSL	LIGSHIY	227
Kir2.1	218	RKSH	LVEAHVR	228
Kir2.2	219	RKSH	LVEAHVR	229
Kir2.3	209	RKSH	LVEAHVR	220
Kir2.4	223	RRSH	LVEAHVR	233
Kir3.1	219	RNSH	MVSAQIR	229
Kir3.2	228	RNSH	LVEASIR	238
Kir3.3	196	RSSH	LVEASIR	206
Kir3.4	225	RNSH	LVEASIR	235
Kir4.1	204	RKSL	LIGCQVT	214
Kir4.2	203	RKSL	LIGCQLS	213
Kir5.1	207	RPNH	VVEGTVR	217
Kir6.1	216	RKSM	LISASVR	226
Kir6.2	206	RKSM	LISATIH	216
Kir7.1	195	RPSPL	LTSVRVS	205



## MATERIAL AND METHODS

### ***In vitro* RNA transcription and *Xenopus laevis* oocyte injection**

Human Kir2.3 (IRK3) cDNA constructs were subcloned into the pGEM-HE vector by previous laboratory members in order to generate transcripts for expression in *Xenopus laevis* oocytes (4). The Kir2.3-pGEM-HE construct was amplified using supercompetent XL1-Blue *E. coli* (Stratagene, La Jolla, CA) and isolated using a miniprep kit (Fermentas, Glen Burnie, MD).

Prior to cRNA *in vitro* transcription, amplified Kir2.3-pGEM-HE was linearized at the 3' end before the 3' untranslated region with *NheI* digestion overnight at 37°C. Kir2.3 cRNA was *in vitro* transcribed using T7 polymerase (Ambion, Austin, TX). Size and integrity of cRNA was confirmed by electrophoresis on 1.2% agarose gel using denaturing buffer (1X MOPS / formaldehyde). Oocytes, prepared through vigorous collagenase digestion, were injected with 2-4 ng of Kir2.3 cRNA. Injection pipettes were made from borosilicate glass (WPI, Sarasota, FL) using a Sutter P-97 microelectrode puller and were manually cut to produce tips of ~12  $\mu$ m diameter.

### **Photocaging of soluble dioctanyl PIP<sub>2</sub> (diC8)**

Our collaborator from North Carolina State University, Dr. Deiters with his coworkers, first solubilized PtdIns-(4,5)-P<sub>2</sub> 1,2-dioctanoyl (PIP<sub>2</sub>) sodium salt (0.5 mg) in 390 mL of ddH<sub>2</sub>O

at pH 4.56. The nitrobenzyl caging group in diethyl ether was added to the reaction and stirred in the dark. After eight hours, the diethyl ether was removed and the remaining mixture was washed with diethyl ether five more times to remove the excess caging group. Lastly, the aqueous layer was filtered by washing with ddH<sub>2</sub>O and the product was concentrated *in vacuo* to yield solid mixtures of singly and doubly caged-diC8. The caged-diC8 mixture [Fig. 11] was stored in a light resistant container and was aliquoted in Fluoride/Vanadate/Pyrophosphate (FVPP: 96 mM KCl, 5 mM EDTA, 10 mM HEPES, 5 mM NaF, 3 mM Na<sub>3</sub>VO<sub>4</sub>, 10 mM Na<sub>2</sub>PO<sub>7</sub>) solution and stored at -20°C prior to use.

### **Preparation of long chain PIP<sub>2</sub> (aa-st PIP<sub>2</sub>)**

L-a-phosphatidylinosito-4,5-bisphosphate (Avanti, Alabaster, AL) was aliquoted and dried using a SpeedVac. The aliquoted amounts were added to a 0.5 mL ND96K solution (91 mM KCl, 1 mM NaCl, 1 mM MgCl<sub>2</sub>, and 5 mM HEPES/KOH), vortexed then sonicated for 12 minutes for two rounds with a 5-minute resting interval in between. The aliquots were then added to 5 mL of FVPP solution, and vortexed then sonicated as described to create a 10 μM long chain PIP<sub>2</sub> solution.

### **Whole-cell recordings and measurements**

Whole-cell recordings [Fig. 7] in *Xenopus laevis* oocytes were made 36-48 hours after cRNA injection. Currents were recorded using two-electrode voltage clamp. Electrodes were filled with 1% agarose in 3 M KCl to prevent leakage of KCl into the oocytes. Electrodes were

pulled to a resistance less than 2 M $\Omega$ . Kir2.3 currents were recorded in high potassium (HK) ND96K solution (as described earlier).

A voltage ramp protocol from -100 mV to 100 mV was applied at one second intervals, and currents corresponding to -100 mV were plotted as a function of time to produce time course relationships. Potassium currents were blocked by 3 mM BaCl<sub>2</sub> in ND96K solution. The leak current was approximated as current passing through the oocyte when the barium solution was perfused and subtracted from the total current measured (3). Whole-cell recordings were obtained using an Axopatch amplifier using Axon 8.1 software (Axon Instruments, Union City, CA). Electrodes were pulled to resistance values between 750 k $\Omega$  – 1.2 M $\Omega$ . The whole-cell recordings from oocytes were carried out 36-48 hours after injection. Data were analyzed and graphed using Clampfit 9.0 (Molecular Devices, Sunnyvale, CA) and Origin 7.0 software (OriginLab, Northampton, MA).

### **Macropatch recordings and measurements**

Macropatch recordings in *Xenopus laevis* oocytes were obtained from manually devitellinized oocytes. All experiments created inside-out patches by gently touching the exterior of the oocyte with the electrode and applying gentle negative pressure [Fig. 8]. Data were collected with the use of an Axon 8.1 patch-clamp amplifier and pCLAMP data acquisition software (Molecular Devices, Sunnyvale, CA). Electrodes were made as previously described except the resistance was between 700 k $\Omega$  to 1.2 M $\Omega$ .



In all macropatch experiments [Fig. 9], FVPP (as described earlier) was used as the bathing solution to inhibit lipid phosphatases and prevent rapid rundown of current due to PIP<sub>2</sub> hydrolysis. Poly-l-lysine (Sigma), with a molecular weight ranging between 30-60 KDa was dissolved in FVPP and used as a scavenger for PIP<sub>2</sub>. Oocytes were also perfused with the following mixtures diluted in FVPP: 2 µg/mL poly-L-lysine, 10 µM aa-st PIP<sub>2</sub>, 50 µM diC8, 50 µM caged-diC8 provided by Dr. Deiters and co-workers. Dr. Tang performed a number of the final experiments to test the effects of UV irradiation on caged-diC8 as well as to confirm results on the non-irradiated caged-diC8.

As with whole-cell currents, a voltage ramp protocol from -100 mV to 100 mV was applied at one-second intervals, and current amplitudes were measured at -100 mV with a sampling rate of 4 kHz. Data were analyzed and graphed using Clampfit and Origin software.

### **Irradiation of caged-diC8 in macropatch recordings**

During macropatch experiments, caged-diC8 was irradiated using a 23 W lamp (UVP, Upland, CA) adjusted to emit 365 nm UV waves (near the maximum absorption wavelength of the diazo-caging groups conjugated to diC8) [Fig. 10]. Due to patches tearing upon direct exposure to UV light, caged-diC8, housed in a plastic syringe, was irradiated at the reservoir placed approximately 40 cm above the macropatch setup. The UV lamp was held approximately 5-10 cm away from the reservoir for 30-60 seconds. Similarly, non-modified diC8 was also irradiated as described to observe whether the UV light had any direct influence on uncaged-diC8 itself.

## Statistics

In the summary data, (Fig. 13B and Fig 14B) error bars in the figures represent SEM. For clarity, the mean of the average currents ( $\mu\text{A}$ ) was normalized to that of current across cell-attached patches. One-way repeated-measures ANOVA were performed, and pairwise comparisons were made by Student-Newman-Keuls method with an overall significance level of  $P < 0.05$  in SigmaStat 3.11 (Systat) to assess whether the perfused reagent elicited significantly different current levels relative to the patch in the cell-attached configuration.

**Figure 7. A schematic demonstrating inwardly-rectifying whole-cell potassium currents in *Xenopus laevis* oocytes using the ramp protocol.** When a voltage ramp protocol from -100 mV to +100 mV is applied to the oocyte membrane, it changes the electrical driving force across the membrane, rapidly altering the membrane potential linearly. The length and direction of the arrows correspond to net  $K^+$  ion movement and direction of movement across the oocyte membrane. Concentration of  $K^+$  ions are assumed to be equal across the membrane (roughly 90 mM), contributing to 0 chemical driving force across the membrane. **Top.** Voltage ramp protocol applied to the oocyte. **Bottom-left:** Schematic shows robust net inward current corresponding to hyperpolarizing voltage of the ramp protocol (-100 mV). **Bottom-middle:** Schematic shows no net movement of  $K^+$  ions (at 0 mV, absence of electrical driving force). **Bottom-right:** Schematic shows significantly less net outward movement of  $K^+$  ions regardless of application of symmetric depolarizing current (+100 mV) across the membrane.

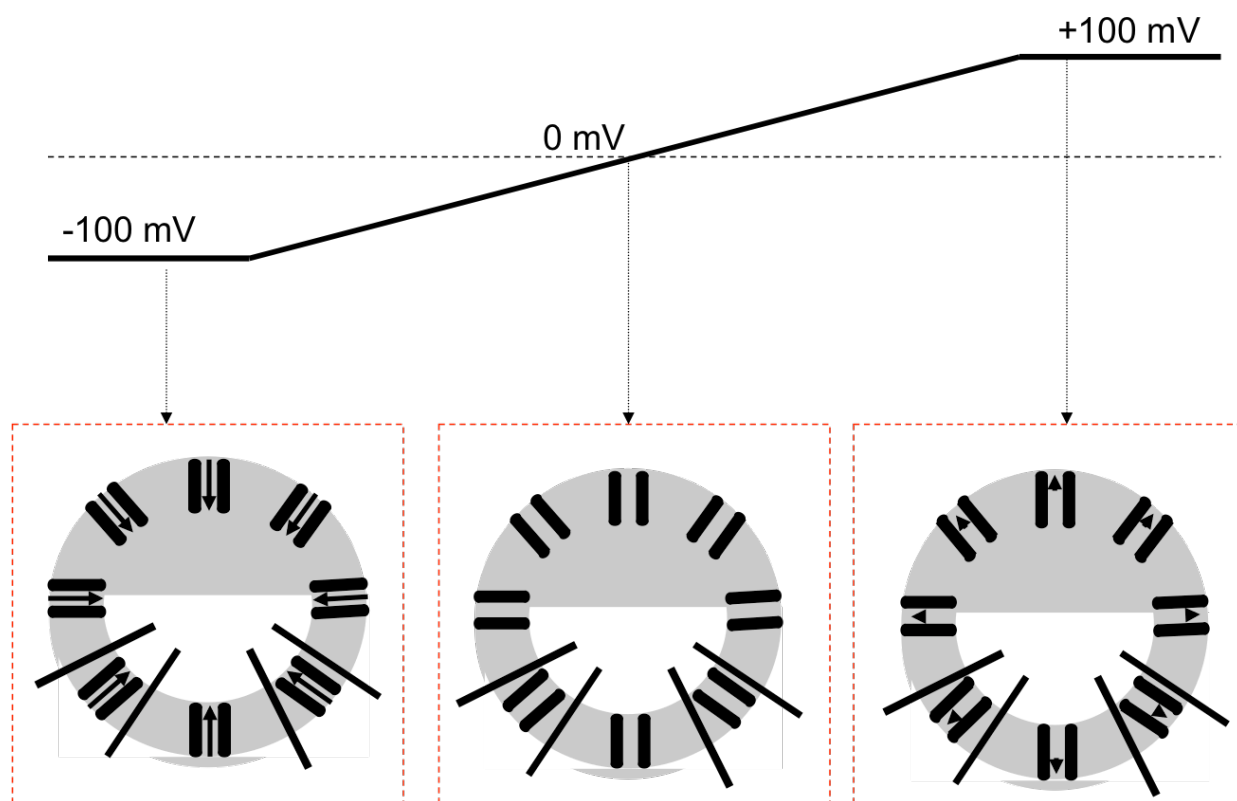


**Figure 8. A schematic of cell-attached (C/A) and inside-out (I/O) macropatch setup.**

**A.** A cell-attached macropatch setup is made by gently touching the exterior of devitellinized oocyte with the electrode and applying gentle negative pressure forming a giga-seal. **B.** Subsequently, the inside-out patch could be setup by pulling the electrode gently away from the oocyte membrane.

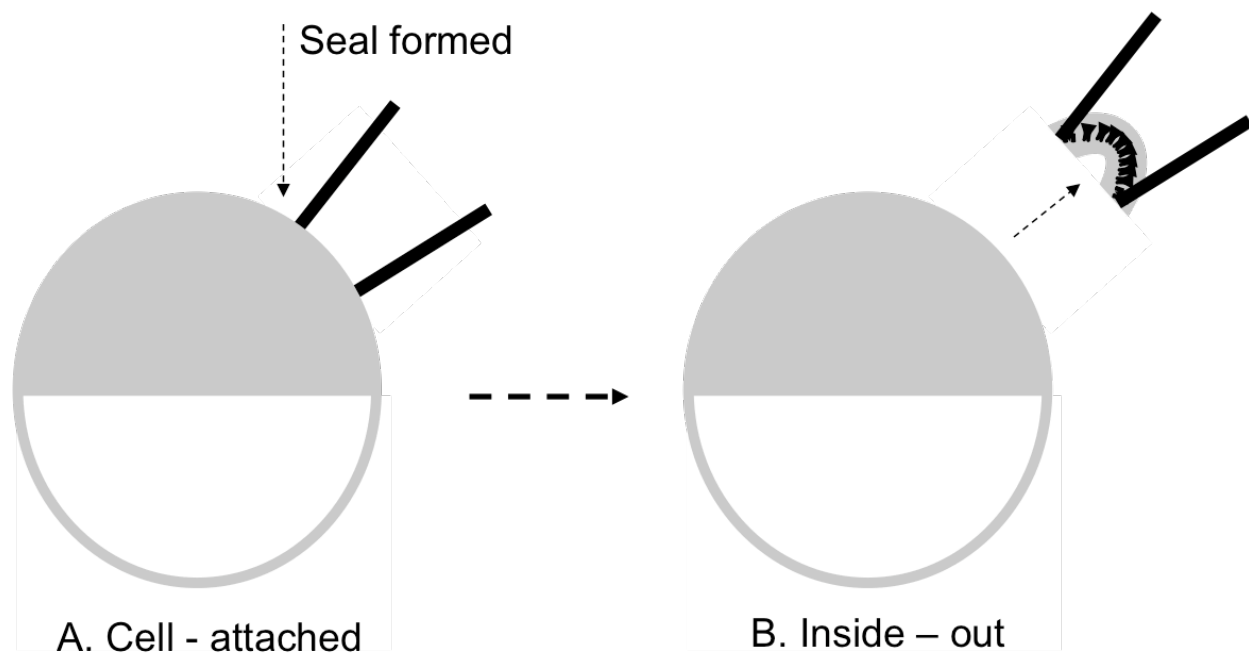
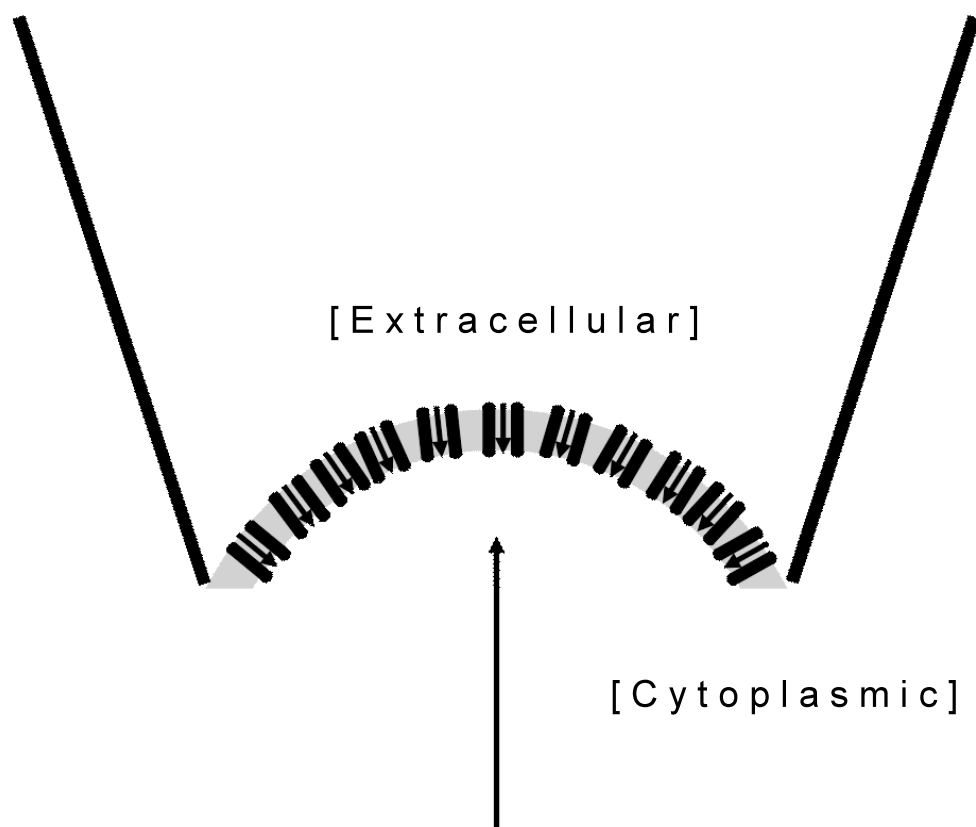


**Figure 9. Inside-out (I/O) patch gives us external control over cytoplasmic conditions.** The inside-out patches afford us with tremendous versatility in searching for cytoplasmic regulators of channel function. The schematic shows inward movement of  $K^+$  ions in response to hyperpolarizing conditions induced by the voltage clamp. Although candidate extracellular factors can be added to the inside of the electrode, it affords very little opportunity for dynamic electrophysiological experiments while one can easily manipulate the cytoplasmic conditions through selective perfusion of candidate co-factor(s).



Perfusion of diC8, caged-diC8, poly-L-lysine, FVPP



**Figure 10. Activating photocaged-diC8 with ultraviolet (UV) irradiation.** A simplified schematic describing the doubly caged (inactive) and uncaged (active) state of doubly caged-diC8. Red boxes with “X” inscribed is a simplified schematic of diazo groups that were conjugated to diC8. **A.** Caged-diC8. Negative charges on phosphate groups are protected by the cages. **B.** Uncaged-diC8. Negative charges on phosphate groups are not exposed and ready to interact with effectors as irradiation bends caging group away from the acidic negative charges.

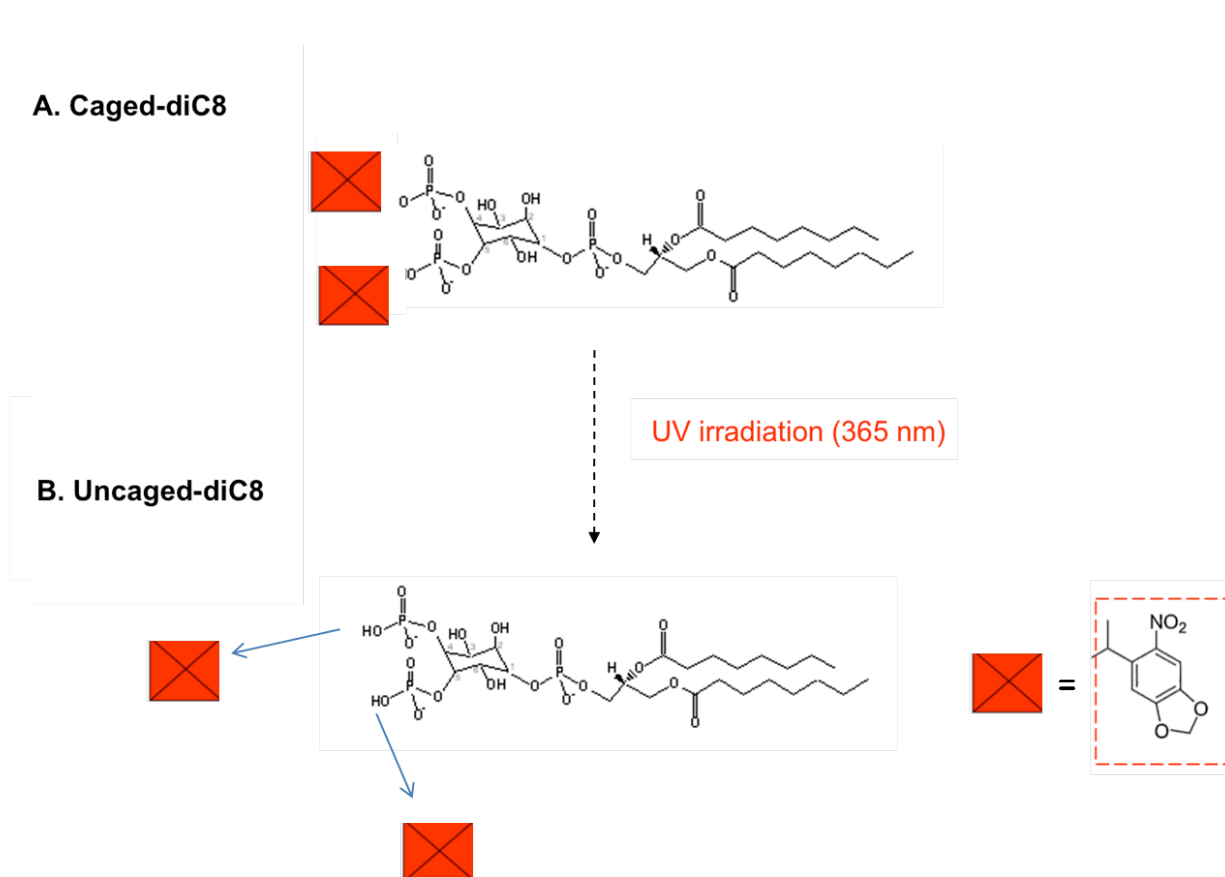
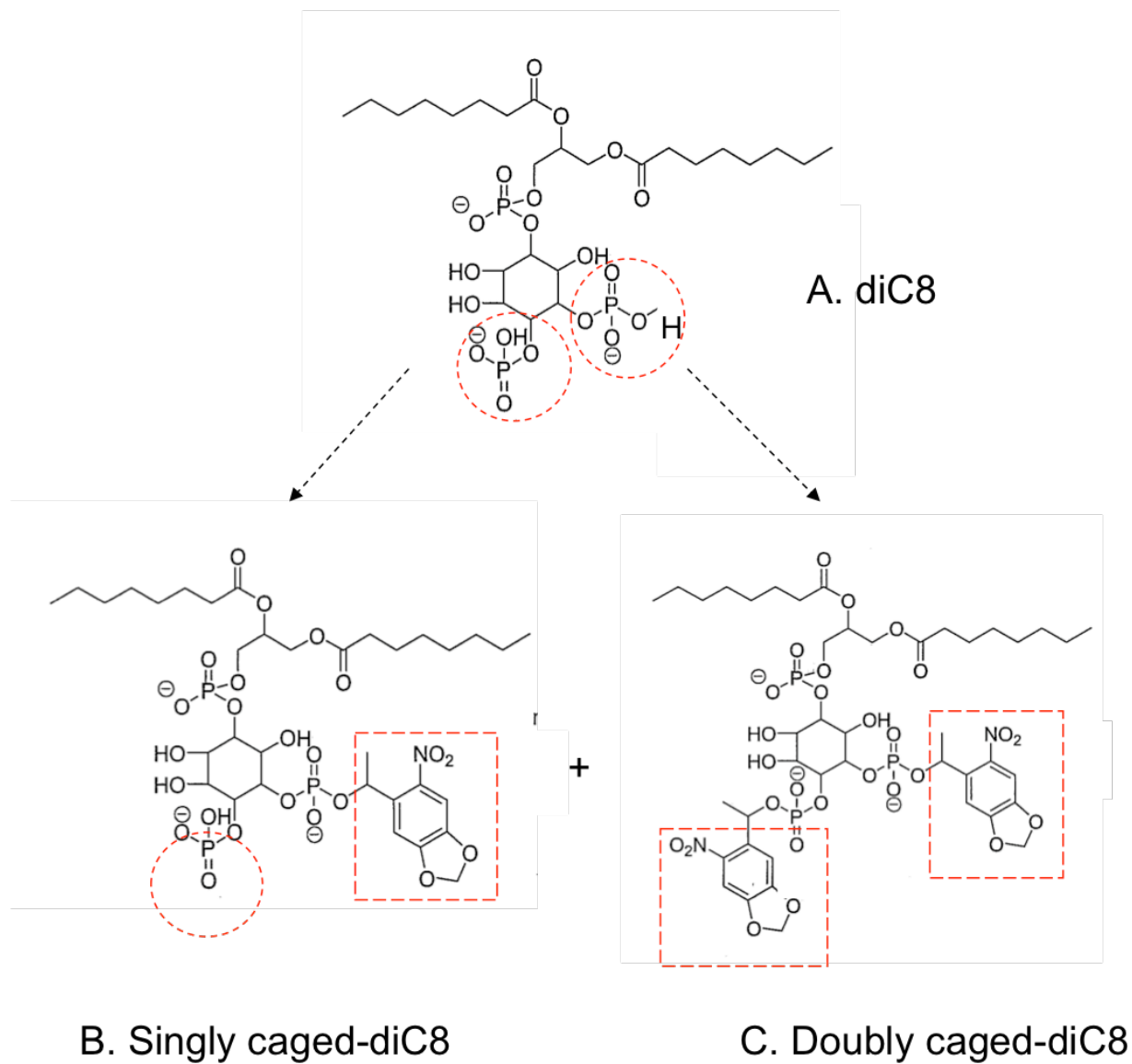


**Figure 11. A schematic of diC8 and singly and doubly photocaged-diC8.** The nitro-benzyl caging group in diethyl ether conjugated to (A) diC8 in the dark to yield (B) singly and (C) doubly caged-diC8.



## RESULTS

### **Kir2.3 (IRK3) channel gives rise to Ba<sup>2+</sup> blocked inwardly rectifying whole-cell K<sup>+</sup> current**

As described in previous heterologous expression experiments, *Xenopus* oocytes were injected with *in vitro* transcribed human Kir2.3 cRNA, and membrane currents were recorded 36-48 hours later using two-electrode voltage clamp. Oocytes were perfused with high potassium (HK) solution ND96K containing 96 mM KCl. A voltage ramp protocol from -100 mV to 100 mV was applied to the membrane at one-second intervals. The magnitude of the hyperpolarization-induced currents (at -100 mV) was plotted as a function of time.

At -100 mV, uninjected oocytes yielded 1-2  $\mu$ A of inward current (data not shown), indicative of trace amounts of endogenously expressed inwardly rectifying channels, while oocytes injected with Kir2.3 cRNA produced currents of mostly 20-25  $\mu$ A [Fig. 12A]. Perfusion of 2 mM BaCl<sub>2</sub> in HK solution blocked nearly 95% of the inward potassium current [Fig. 12A] in agreement with previous studies.

Current-voltage relationships of Ba<sup>2+</sup>-sensitive currents from Kir2.3 injected oocytes confirmed the inwardly rectifying properties of Kir2.3 [Fig 12B]. These results confirm previous studies that Kir2.3 produces a robust inwardly rectifying potassium current that is sensitive to barium block.

**Long chain PIP<sub>2</sub> (aa-st PIP<sub>2</sub>) and soluble dioctanoyl PIP<sub>2</sub> (diC8) rescue Kir2.3 currents in excised macropatches.**

*Xenopus* oocytes were injected with *in vitro* transcribed Kir2.3 cRNA and were allowed to express the channel for 36-48 hours. The injected oocytes were devitellinized manually through the use of forceps because the vitelline membrane impedes seal formation, and a microelectrode was carefully juxtaposed to the oocyte plasma membrane with gentle negative pressure to form a GΩ-seal. From the cell-attached configuration, a patch was excised from the oocyte to generate an inside-out macropatch, exposing the extracellular side of the membrane partition to the HK ND96K solution contained in the microelectrode, and the cytoplasmic side to the perfusion solution. This mode of the patch-clamp technique is ideal for testing intracellular modulators of ion channel activity by bath perfusion.

When hyperpolarized to -100 mV, inward current magnitudes of 200-1000 pA were recorded in macropatches expressing Kir2.3 while 20-30 pA currents were measured in uninjected oocytes [data not shown]. As described in previous experiments, the inward current recorded in macropatches usually increased or decreased prior to run-down upon excision from the oocyte in the cell-attached to inside-out patch configuration reflecting the immediate changes in cytoplasmic concentration of potassium. The eventual run-down (data not shown) as the patch was held in inside-out setup represented the dephosphorylation of endogenous, membrane delimited PIP<sub>2</sub> in the patch

Addition of the naturally occurring long chain arachidonic acid-stearyl (aa-st) PIP<sub>2</sub> (10 μM) significantly increased the activity of injected patches 2-fold [Fig. 13B]. Perfusion with a solution containing Fluoride/Vanadate/Pyrophosphate (FVPP), that inhibits lipid phosphatases,

maintained channel activity [Fig. 13A]. Perfusion of poly-L-lysine acutely reversed the action of aa-st PIP<sub>2</sub> and dramatically inhibited the inward current magnitude of macropatches expressing Kir2.3 [Fig. 13A] exhibiting PIP<sub>2</sub> scavenging behavior as described by previous work (Lopes, 2002). The inhibitory effect of poly-L-lysine was also washed out upon continuous perfusion of aa-st PIP<sub>2</sub> (data not shown).

The soluble phosphoinositide form diC8 (50 μM) also restored the inward current elicited by Kir2.3 channels by roughly 85-90% of the current observed in cell-attached patches at -100 mV [Fig 14B]. DiC8 perfusion reversed the inhibitory action of poly-L-lysine [Fig. 14A], similar to the action of long-chain PIP<sub>2</sub> (aa-st PIP<sub>2</sub>) but with faster activation kinetics [Figs. 13 and 14] as well as deactivation kinetics. These observations are in agreement with previous experiments that showed how readily diC8 can diffuse out of the membrane compared to its endogenous long chain analog [ 5 ].

### **Caged-diC8 is able to restore inward Kir2.3 currents.**

While the initial results (n = 3) suggested that caged-diC8 had no effect on inward Kir2.3 current [Fig. 15] in macropatches, they were inconclusive due to the instability of excised patches during these experiments. While in most cases, caged-diC8 seemed to have little or no effect on Kir2.3 activation, patches tended to break before convincing activation with control active PIP<sub>2</sub> could be confirmed. Dr. Qiong-yao Tang's subsequent experiments succeeded in showing that caged-diC8 (~50 μM) was able to restore the current activity by 90% of the magnitude of inward current measured for the cell-attached configuration following poly-L-

lysine inhibition [Fig. 17]. Interestingly, caged-diC8 activation produced highly fluctuating currents [Fig. 16A] relative to currents elicited by unmodified diC8 [Figs 14A and 15].

**UV-irradiation inactivates caged-diC8, reproducing a fraction of the inward Kir2.3 currents restored by caged-diC8.**

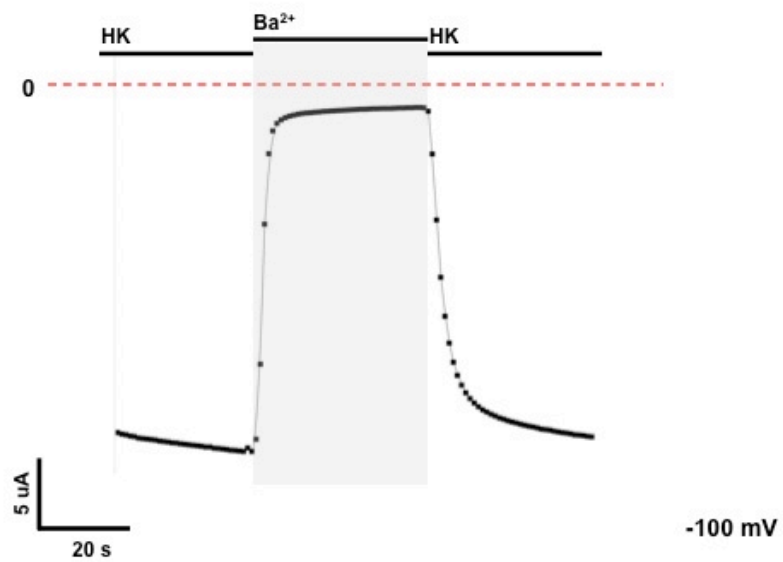
Irradiating the macropatch directly with a 365 nm UV wavelength to de-cage the caged-diC8, often destroyed the patch while generating an electrical noise that complicated the analysis of electrical recordings (data not shown). Instead, Dr. Qiong-yao Tang irradiated the reservoir containing caged-diC8 for 60-90s at an approximate 10 cm distance from the inside-out patch prior to perfusion. Surprisingly, the irradiation of caged-diC8 yielded currents that were 45% compared to that of caged-diC8 currents [Fig. 17].

Interestingly, irradiation of caged-diC8 also seemed to reduce the high fluctuations typical of currents elicited by non-irradiated caged-diC8 and to elicit lower currents than the non-irradiated caged-diC8 [Fig 16A].



**Figure 12. Expression of Kir2.3 in *Xenopus laevis* oocytes gives rise to robust whole-cell inwardly rectifying potassium current.** **A.** Representative time course of Kir2.3 activity. At hyperpolarizing conditions using (-100 mV), Kir2.3 elicits robust inward current (~25  $\mu$ A) in high-potassium (HK) 90 mM solution, while the perfusion of barium chloride (2 mM) nearly abrogated the whole-cell activity of the channel. **B.** Current-voltage relationships of Ba<sup>2+</sup>-sensitive currents (n = 7) from Kir2.3 cRNA injected oocytes show the inwardly rectifying properties of Kir2.3 [Fig. 7].

A.



B.

Kir2.3 I-V Plot ( n = 7 )

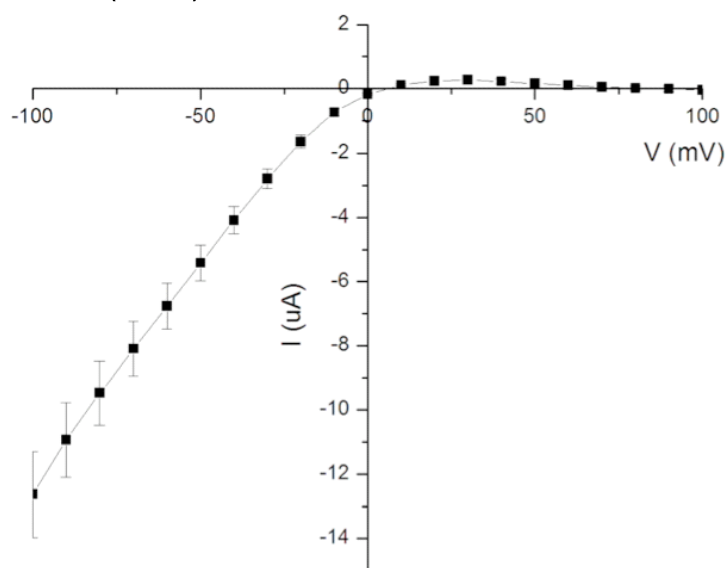
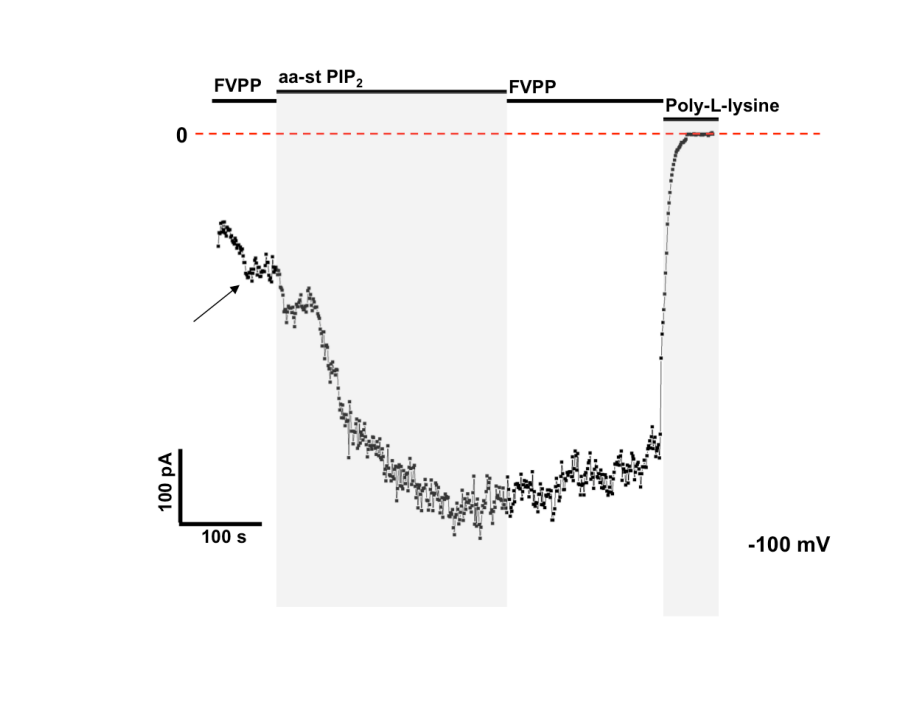


**Figure 13. Application of long chain PIP<sub>2</sub> (aa-st PIP<sub>2</sub>) to the cytoplasmic side of inside-out oocyte macropatch activates the Kir2.3 current.** Addition of long chain arachidonic acid-stearyl (aa-st) PIP<sub>2</sub> (10 μM) significantly increased Kir channel activity. **A.** Representative trace of Kir2.3 activity. Time course shows that perfusion with FVPP maintained channel activity, while subsequent application of long chain PIP<sub>2</sub> activated Kir2.3 currents; addition of poly-L-lysine (2 ug/mL) inhibited the inward current magnitude of macropatches expressing Kir2.3. **B.** Summary of traces shows significant increase of Kir2.3 activity upon application of aa-st PIP<sub>2</sub> (*P* < 0.03).

A.



B.

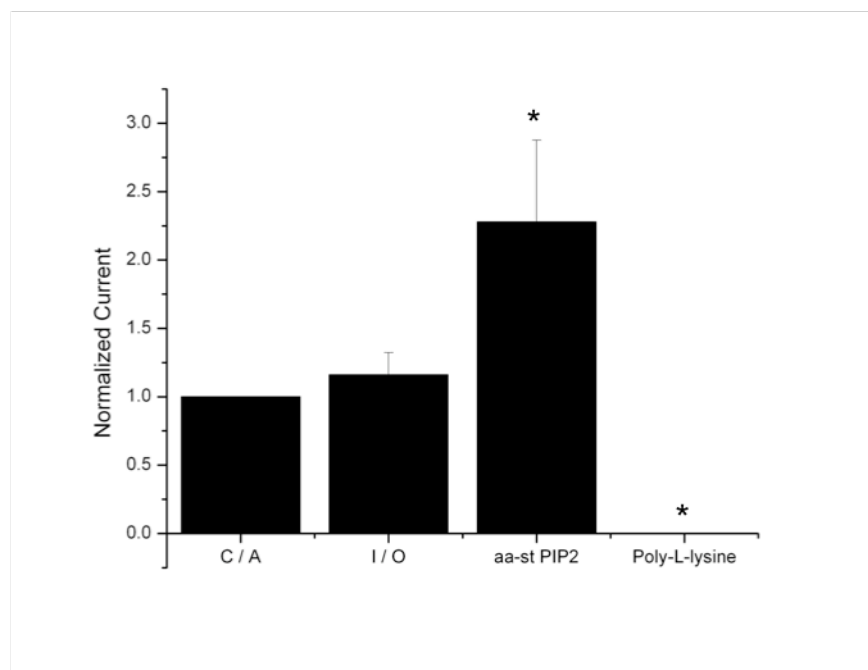
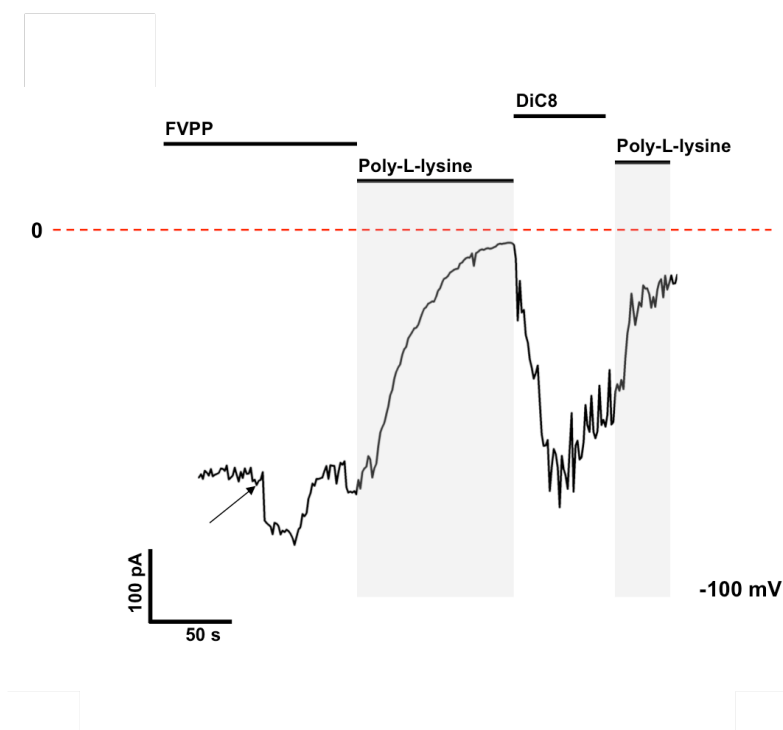


**Figure 14. Application of dioctanoyl PIP<sub>2</sub> (diC8) to the cytoplasmic side of inside-out oocyte macropatch rescues Kir2.3 current.** Addition of diC8 (50  $\mu$ M) significantly increased channel activity. **A.** Representative tracing of Kir2.3 activity. Time course shows that perfusion with FVPP maintained channel activity. While subsequent application of poly-L-lysine inhibited the inward current, ensuing application of diC8 rescued Kir2.3 current. **B.** Summary of traces show significant rescue of Kir2.3 activity upon application of diC8 ( $P < 0.001$ ) .

A.



B.

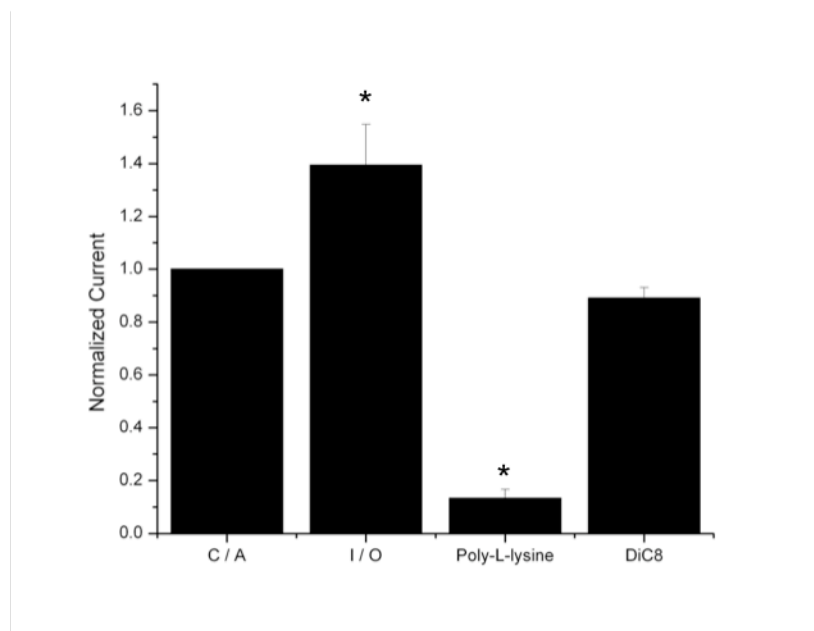


**Figure 15. Preliminary finding shows that caged-diC8 is inactive.** Addition of caged-diC8 was not able to maintain the activation of the Kir2.3 current following their activation by the unmodified diC8.

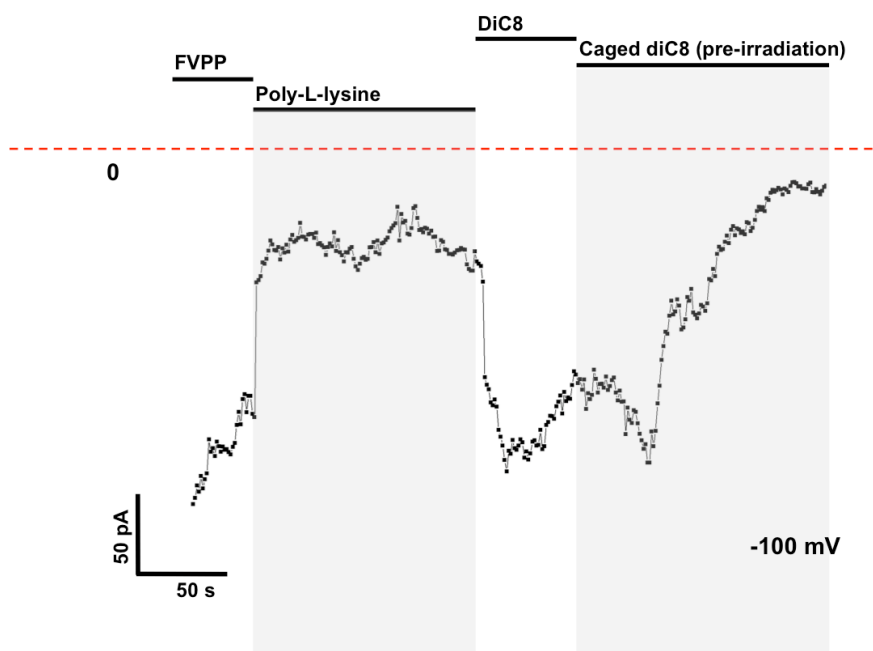




**Figure 16. Caged-diC8 activates the Kir2.3 current, while irradiation (de-caging) limits the effectiveness of caged-diC8.** **1.** Reactivation of Kir2.3 channels by caged-diC8 (50  $\mu\text{M}$ ) following depletion of endogenous  $\text{PIP}_2$  by poly-L-lysine (300  $\mu\text{g/ml}$ ). **2A:** Traces show the reactivation by caged-diC8 (50  $\mu\text{M}$ ) before and after UV irradiation. Poly-L-lysine (300  $\mu\text{g/ml}$ ) was applied after the current was relatively stable; the kinetics of the current reactivated by caged-diC8 can be fitted by a single exponential function.  $T_{50}$  represents the time to reach 50% activation. **Dashed line:** zero current, **Arrow:** application of poly-L-lysine (poly-Lys); **Horizontal bar:** indicates application of caged-diC8 before and after UV irradiation. **3B and 3C:** representative ramp traces from the time points indicated by numbers in A: 3B before UV and 3C after UV irradiation.

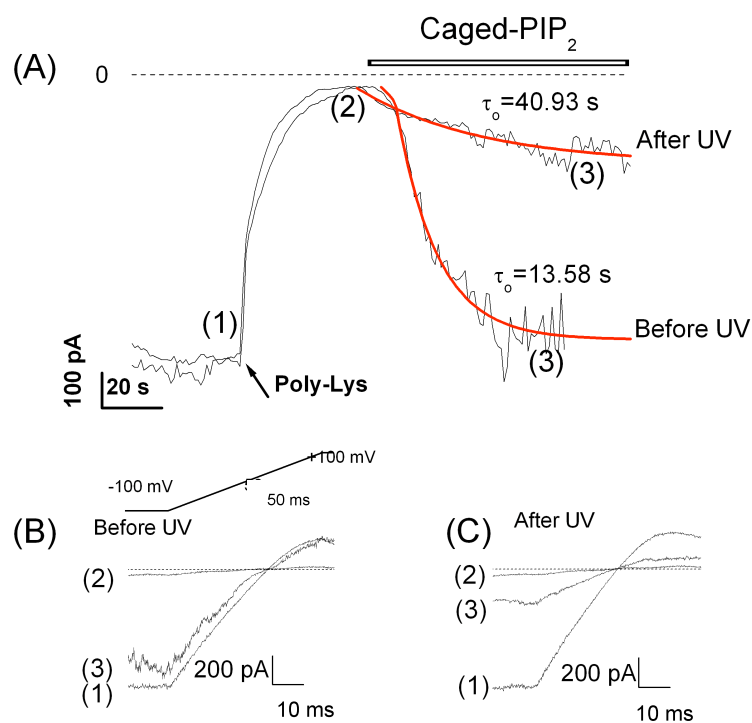
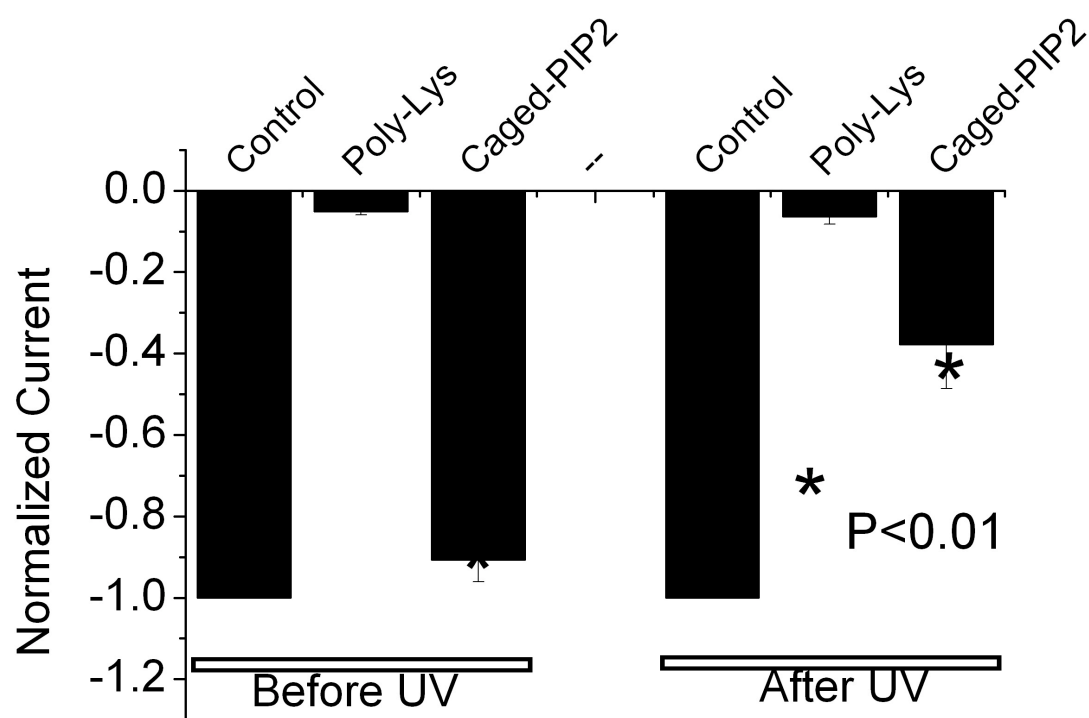


**Figure 17. Summary data: caged-diC8 effect before and after UV irradiation.** Kir 2.3 currents are normalized and plotted together with the effect of poly-L-lysine (poly-Lys) before and after UV irradiation.



## DISCUSSION AND FUTURE DIRECTIONS

The purpose of this study was to develop a novel tool (photocaged dioctanoyl PIP<sub>2</sub>) for studying the effects of PI(4,5)P<sub>2</sub> that could be activated at will (e.g. upon UV irradiation and de-caging). Availability of such a molecular tool could be utilized in whole-cell systems, where microinjection of inactive caged PIP<sub>2</sub> would not interfere with the cell's electrical activity but upon de-caging the effects of PIP<sub>2</sub> could be assessed. Unavailability of a caged PIP<sub>2</sub> has forced past studies to focus on excised patch settings. While shortening the fatty acid chains of endogenous long chain PIP<sub>2</sub> to an eight-carbon long chain in dioctanoyl PIP<sub>2</sub> (diC8) has been used effectively to study ion channel modulation by PIP<sub>2</sub> in inside-out patches, their application to whole-cell systems has been severely limited. Although we have much control over the PIP<sub>2</sub> delivery in inside-out patch settings by simply altering perfusion solutions, the application of PIP<sub>2</sub> into the whole cell through the microelectrode is slow and inefficient as the phospholipid sticks to the glass electrode and does not permit us to look at the functional effects of PIP<sub>2</sub> dynamically.

We were motivated to increase the degree of external control we have in whole-cell systems (as in excised patches) through the addition of a light activated switch on diC8 in collaboration with Dr. Deiter's lab at North Carolina State University. Here, we have tested the functional effects of caged and uncaged diC8 in an established macropatch system expressing

Kir2.3 to verify whether the 1) caging inactivates PIP<sub>2</sub> function and 2) decaging through UV irradiation restores PIP<sub>2</sub> function. Although initial experiments suggested that caging diC8 reduces its activity [Fig. 15], our subsequent observations have been contrary to these findings as well as to our expectations. We show that caged-diC8 behaves similarly to unmodified diC8 while de-caging diC8 through UV irradiation produces a less effective PIP<sub>2</sub> to activate Kir2.3 currents [Figs. 16 and 17].

Before we tested the functional effects of photocaged-diC8, we reproduced experiments on Kir2.3 expression through the use of two-electrode-voltage clamp (TEVC) technique and macropatch experiments with long chain PIP<sub>2</sub> (aa-st PIP<sub>2</sub>) and diC8 [Figs. 12, 13, 14] to verify past observations and prepare to test the photocaged-diC8. The TEVC experiments [Fig 12] verified that the Kir2.3 construct can be successfully expressed to record robust inwardly rectifying potassium currents [Fig 12B]. Macropatch experiments with long chain PIP<sub>2</sub>, diC8, and poly-L-lysine verified the activating effects that PIP<sub>2</sub> had on Kir2.3 as well as providing us with information to compare and contrast our results with the effects of photocaged-diC8.

Our initial experiments suggested that caged-diC8 did not activate Kir2.3 currents [Fig. 15]. Other trials have reproduced these results, however, patches broke soon after the perfusion of caged-diC8 not precluding the possibility of current recovery at a slower kinetic rate. Indeed, Dr. Qiong-yao Tang's subsequent experiments with caged-diC8 showed more convincingly (n = 5) that in conditions where patches could withstand perfusion longer, caged-diC8 was able to restore Kir2.3 current like unmodified diC8, however with much slower kinetics [Fig. 16A]. We also observed in both initial and subsequent experiments testing caged-diC8 that the Kir2.3 current fluctuates much more than in diC8. This observation is consistent with the notion that the

perfused caged-diC8 is a mixture of doubly or singly caged-diC8: it is possible that the singly caged-diC8 still retains functional activity haphazardly and this may contribute to the fluctuating current that is absent in the unmodified, fully active diC8.

Our attempts to de-cage diC8 through direct irradiation of the macropatch at 365 nm wavelength using a 23W UV lamp were met with oscillating electrical noise that complicated analysis of recordings as well as resulting in macropatch break down (data not shown). Therefore, we elected to irradiate the reservoir of caged-diC8 to test its functional effect on Kir2.3 currents. Contrary to our expectations, irradiated caged-diC8 (decaged-diC8) elicited ~30% of the current that could be recovered by caged-diC8 [Fig. 17]. To rule out the possibility that irradiation itself may have damaged caged-diC8 nonspecifically, we are in the process of irradiating the reservoir of unmodified diC8 to test whether it has any effect on its function.

Presently, further experiments with caged-diC8 in macropatches are required prior to their use in the whole-cell configuration. In particular, we could modify the caged-diC8 mixture so that most of the mixture is doubly caged to avoid further complications in our interpretation of results. We can also invest in a more ideal (lower intensity), focused source of UV-irradiation to limit its damaging effect on the macropatches and potentially on diC8 as well. The focusing of UV irradiation will also be a nice modification if future experiments attempt to spatially modulate diC8 function in a whole-cell system.

Overall, the photocaging of diC8 deserves further development. If our modifications allow us to externally control the activation of diC8 with UV light, we will need to test whether the caging affects diC8 interaction with other cytoplasmic factors such as phosphatases and kinases. If successfully implemented in macropatches, photocaged-diC8 will equip us with the

tremendous potential to study whole-cell electrical activity simultaneously with the activation of diC8. The caging groups can also be modified so that they can be switched, “OFF” at a wavelength that is distinct from the “ON” wavelength. The addition of fluorophores to photocaged-diC8 may also be used to assay the interaction between ion channel and PIP<sub>2</sub> concomitantly.



## LITERATURE CITED

1. **Banaszynski LA, Chen LC, Maynard-Smith LA, Ooi AG, and Wandless TJ.** A rapid, reversible, and tunable method to regulate protein function in living cells using synthetic small molecules. *Cell* 126: 995-1004, 2006.
2. **Buskirk AR and Liu DR.** Creating small-molecule-dependent switches to modulate biological functions. *Chem Biol* 12: 151-161, 2005.
3. **Chan KW, Langan MN, Sui JL, Kozak JA, Pabon A, Ladias JA, and Logothetis DE.** A recombinant inwardly rectifying potassium channel coupled to GTP-binding proteins. *J Gen Physiol* 107: 381-397, 1996.
4. **Du X, Zhang H, Lopes C, Mirshahi T, Rohacs T, and Logothetis DE.** Characteristic interactions with phosphatidylinositol 4,5-bisphosphate determine regulation of kir channels by diverse modulators. *J Biol Chem* 279: 37271-37281, 2004.
5. **Fan Z and Makielski JC.** Anionic phospholipids activate ATP-sensitive potassium channels. *J Biol Chem* 272: 5388-5395, 1997.
6. **Gamper N and Shapiro MS.** Regulation of ion transport proteins by membrane phosphoinositides. *Nat Rev Neurosci* 8: 921-934, 2007.
7. **Hamill OP, Marty A, Neher E, Sakmann B, and Sigworth FJ.** Improved patch-clamp techniques for high-resolution current recording from cells and cell-free membrane patches. *Pflugers Arch* 391: 85-100, 1981.

8. **Hilgemann DW.** Local PIP<sub>2</sub> signals: when, where, and how? *Pflugers Arch* 455: 55-67, 2007.
9. **Hilgemann DW and Ball R.** Regulation of cardiac Na<sup>+</sup>,Ca<sup>2+</sup> exchange and KATP potassium channels by PIP<sub>2</sub>. *Science* 273: 956-959, 1996.
10. **Hille B.** *Ion channels of excitable membranes.* Sunderland, Mass.: Sinauer, 2001.
11. **Keselman I, Fribourg M, Felsenfeld DP, and Logothetis DE.** Mechanism of PLC-mediated Kir3 current inhibition. *Channels (Austin)* 1: 113-123, 2007.
12. **Lehninger AL, Nelson DL, and Cox MM.** *Lehninger principles of biochemistry.* New York: W.H. Freeman, 2008.
13. **Logothetis DE, Jin T, Lupyan D, and Rosenhouse-Dantsker A.** Phosphoinositide-mediated gating of inwardly rectifying K<sup>+</sup> channels. *Pflugers Arch* 455: 83-95, 2007.
14. **McLaughlin S, Wang J, Gambhir A, and Murray D.** PIP<sub>2</sub> and proteins: interactions, organization, and information flow. *Annu Rev Biophys Biomol Struct* 31: 151-175, 2002.
15. **Padidam M, Gore M, Lu DL, and Smirnova O.** Chemical-inducible, ecdysone receptor-based gene expression system for plants. *Transgenic Res* 12: 101-109, 2003.
16. **Rohacs T, Chen J, Prestwich GD, and Logothetis DE.** Distinct specificities of inwardly rectifying K<sup>+</sup> channels for phosphoinositides. *J Biol Chem* 274: 36065-36072, 1999.
17. **Rohacs T, Lopes CM, Jin T, Ramdya PP, Molnar Z, and Logothetis DE.** Specificity of activation by phosphoinositides determines lipid regulation of Kir channels. *Proc Natl Acad Sci U S A* 100: 745-750, 2003.
18. **Suh BC and Hille B.** PIP<sub>2</sub> is a necessary cofactor for ion channel function: how and why? *Annu Rev Biophys* 37: 175-195, 2008.

19. **Tucker SJ and Baukrowitz T.** How highly charged anionic lipids bind and regulate ion channels. *J Gen Physiol* 131: 431-438, 2008.
20. **Xu C, Watras J, and Loew LM.** Kinetic analysis of receptor-activated phosphoinositide turnover. *J Cell Biol* 161: 779-791, 2003.
21. **Young DD and Deiters A.** Photochemical control of biological processes. *Org Biomol Chem* 5: 999-1005, 2007.
22. **Zhang H, He C, Yan X, Mirshahi T, and Logothetis DE.** Activation of inwardly rectifying K<sup>+</sup> channels by distinct PtdIns(4,5)P<sub>2</sub> interactions. *Nat Cell Biol* 1: 183-188, 1999.

## VITA

Junghoon Ha was born on June 30, 1981 in Seoul, South Korea. Mr. Ha immigrated to the United States in July, 1988. He attended Thomas Jefferson High School for Science and Technology in Alexandria, VA, where he graduated with a Jefferson diploma in 2000. In 2004, he received his B.Sc. in Biology from University of Virginia in Charlottesville, VA. During his undergraduate studies, he was trained in molecular biology under the mentorship of Dr. Anthony Spano, Research Scientist in the Biology Department. Thereafter, he was trained as a live-cell imaging microscopist under the mentorship of Dr. Kevin Pfister (2004-2007), an Associate Professor of Cell Biology in the Molecular Cell and Developmental Biology Department at the University of Virginia School of Medicine. Afterwards, he enrolled in Virginia Commonwealth University School of Medicine as a candidate M.S. student in the Physiology and Biophysics Department on Aug. 2007. In the ensuing year, he joined Dr. Logothetis's lab in the summer of 2008 and worked to produce the results that are embodied in this thesis.